Soils and Foundations 2013;53(6):820–834

The Japanese Geotechnical Society

Soils and Foundations

www.sciencedirect.com
journal homepage: www.elsevier.com/locate/sandf

Expanded reliability-based design of piles in spatially variable soil using efficient Monte Carlo simulations

Yu Wang[a,1], Zijun Cao[b,*]

[a]Department of Civil and Architectural Engineering, City University of Hong Kong, Tat Chee Avenue, Kowloon, Hong Kong
[b]State Key Laboratory of Water Resources and Hydropower Engineering Science, Wuhan University, No. 8 Donghu South Road, Wuhan, PR China

Received 3 December 2012; received in revised form 25 June 2013; accepted 24 July 2013
Available online 20 November 2013

Abstract

Inherent spatial variability is considered as a major source of uncertainties in soil properties, and it affects significantly the performance of geotechnical structures. However, research that considers, directly and explicitly, the inherent spatial variability in reliability-based design (RBD) of geotechnical structures is limited. This paper develops a RBD approach that integrates a Monte Carlo Simulation (MCS)-based RBD approach, namely the expanded RBD approach, with random field theory to model, both directly and explicitly, the inherent spatial variability of soil properties in RBD of drilled shafts. The proposed approach is implemented in a commonly-available spreadsheet environment to effectively remove the hurdle of reliability computational algorithms and to provide a user-friendly graphical user interface to practicing engineers. To improve the efficiency and resolution of MCS at small probability levels, the expanded RBD approach is enhanced with an advanced MCS method called "Subset Simulation". Equations are derived for the integration of the expanded RBD approach and Subset Simulation. The proposed approach is illustrated through a drilled shaft design example, and is applied to explore the effects of inherent spatial variability (including the scale of fluctuation and correlation structure) and to evaluate systematically the equivalent variance technique that is commonly used to indirectly model inherent spatial variability in current RBD approaches. It is found that inherent spatial variability significantly affects the RBD of drilled shafts, and its effects are considered in RBD using the proposed approach in a direct and explicit manner. In addition, the results show that the indirect modeling of inherent spatial variability using the equivalent variance technique with the simplified form of variance reduction function in RBD might lead to relatively conservative designs in design practice.

Keywords: Inherent spatial variability; Reliability-based design; Monte Carlo simulation; Subset Simulation; EXCEL spreadsheet; Design practice; IGC: E4; H1

1. Introduction

The properties of geotechnical materials are affected by various factors in natural geological processes, such as parent materials, weathering and erosion processes, transportation agents, conditions of sedimentation, etc. (e.g., Mitchell and Soga, 2005). These factors vary spatially from one location to another, which subsequently lead to inherent spatial variability of geotechnical properties (Vanmarcke, 1977, 1983). Inherent spatial variability has been considered as a major source of uncertainties in soil properties (e.g., Christian et al., 1994; Kulhawy, 1996; Phoon and Kulhawy, 1999a; Baecher and Christian, 2003). It significantly affects the performance of geotechnical structures that, under a probabilistic framework, is commonly measured by the probability of failure p_f (or reliability index β) of geotechnical structures (e.g., Fenton and Griffiths, 2002, 2007; Zhang and Chu, 2009a, b; Wang et al., 2011b;

*Corresponding author. Tel.: +86 27 68774036.
E-mail addresses: yuwang@cityu.edu.hk (Y. Wang), zijuncao3@gmail.com (Z. Cao).
[1]Tel.: +852 3442 7605 ; fax: +852 3442 0427.
Peer review under responsibility of The Japanese Geotechnical Society.

Production and hosting by Elsevier

0038-0806 © 2013 The Japanese Geotechnical Society. Production and hosting by Elsevier B.V. All rights reserved.
http://dx.doi.org/10.1016/j.sandf.2013.10.002

Luo et al., 2012; Zhang and Chen, 2012; Kasama et al., 2012; Teixeira et al., 2012; Kim and Sitar, 2013).

The effect of inherent spatial variability has been, directly and explicitly, incorporated into the probabilistic analysis of geotechnical structures using random field theory in several previous studies (e.g., Fenton and Griffiths, 2002, 2003; Griffiths and Fenton, 2004, 2009; Huang et al., 2010; Wang et al., 2011b; Li et al., 2013). Note that the probabilistic analysis aims to estimate the p_f (or β) for an existing geotechnical structure or a pre-defined design (e.g., Zhang et al., 2011). This is the inverse of the reliability-based design (RBD), which aims to determine an optimal design of geotechnical structures that satisfies a series of pre-defined performance requirements, including target failure probability p_T (or target reliability index β_T) (e.g., Honjo et al., 2010). In current RBD approaches, the inherent spatial variability is commonly addressed through an equivalent variance technique (e.g., Phoon et al., 1995; Klammler et al., 2010; Naghibi and Fenton 2011; Fenton and Naghibi, 2011; Luo et al., 2012). In the equivalent variance technique, the soil property within a statistically homogenous soil mass is characterized by a single random variable that represents the spatial average of the soil property over the soil mass and has a reduced variance due to the spatial averaging (Vanmarcke, 1977, 1983). The equivalent variance technique models the inherent spatial variability in an indirect and implicit manner, and the effect of such an indirect modeling method (i.e., equivalent variance technique) in RBD has not been explored systematically.

This study develops a RBD approach for drilled shafts, which integrates a Monte Carlo Simulation (MCS)-based RBD approach, namely the expanded RBD approach (Wang, 2011, 2013; Wang et al., 2011a), with the random field theory to model, directly and explicitly, the inherent spatial variability of soil properties in RBD of drilled shafts. The proposed approach is implemented in a commonly-available EXCEL spreadsheet environment to effectively remove the hurdle of reliability computational algorithm and to provide a user-friendly graphical user interface to practicing engineers. Then, the effect of indirect modeling of inherent spatial variability using the equivalent variance technique in current RBD approaches is evaluated systematically. In addition, to improve the computational efficiency and resolution of MCS, the expanded RBD approach is further enhanced with an advanced MCS method called "Subset Simulation".

This paper starts with the probabilistic modeling of the inherent spatial variability of soil properties for the drilled shaft design, followed by an introduction to the expanded RBD approach, the Subset Simulation, and their integration. Then, the proposed approach is illustrated through a drilled shaft design example and is applied to explore effects of inherent spatial variability (including the scale of fluctuation and correlation structure) and the indirect modeling of inherent spatial variability using the equivalent variance technique in RBD. In addition, the effect of a key factor (i.e., the so-called "driving variable") in Subset Simulation is also explored. Recommendations are provided for the proper selection of the driving variable when using Subset Simulation in the expanded RBD approach.

2. Inherent spatial variability modeling in RBD

2.1. Random field modeling (RFM)

Random field theory (Vanmarcke, 1977, 1983) is applied in this subsection to model, directly and explicitly, the inherent spatial variability of soil properties in RBD of drilled shafts. Consider, for example, the effective stress friction angle ϕ' in a statistically homogenous soil layer, as shown in Fig. 1. The inherent spatial variability of ϕ' with depth is characterized by a one-dimensional homogenous lognormal random field $\phi'(z_i)$, in which z_i is the depth and ϕ' is a lognormal random variable with a mean $\mu_{\phi'}$ and standard deviation $\sigma_{\phi'}$ (or coefficient of variation $\mathrm{COV}_{\phi'}=\sigma_{\phi'}/\mu_{\phi'}$). In the context of random fields, the spatial correlation between variations of ϕ' at different locations is characterized by the scale of fluctuation and correlation structure (Vanmarcke, 1977, 1983; Li and Der Kiureghian, 1993). Here, the correlation structure is taken as a single exponential correlation function, and the correlation coefficient ρ_{ij} between the logarithms (e.g., $\ln\phi'(z_i)$ and $\ln\phi'(z_j)$) of ϕ' at respective depths z_i and z_j is given by (e.g., Fenton, 1999a, b; Wang et al., 2010a; Cao and Wang, 2013)

$$\rho_{ij}=\exp(-2|z_i-z_j|/\lambda) \tag{1}$$

where λ=scale of fluctuation. As implied by Eq. (1), when $|z_i-z_j|\geq\lambda$, $\ln\phi'(z_i)$ and $\ln\phi'(z_j)$ are effectively uncorrelated (Vanmarcke, 1977, 1983). When $|z_i-z_j|$ is much smaller than λ, $\ln\phi'(z_i)$ and $\ln\phi'(z_j)$ are highly correlated. Note that the approach proposed in this study is general and equally applicable for different correlation structures. The effect of different correlation structures on RBD is further discussed in a later section.

Fig. 1 illustrates a drilled shaft with a diameter B and depth D, and the soil layer surrounding the drilled shaft is divided into N_t sub-layers, each of which has a thickness of d. Note that the soil layer surrounding the drilled shaft is discretized

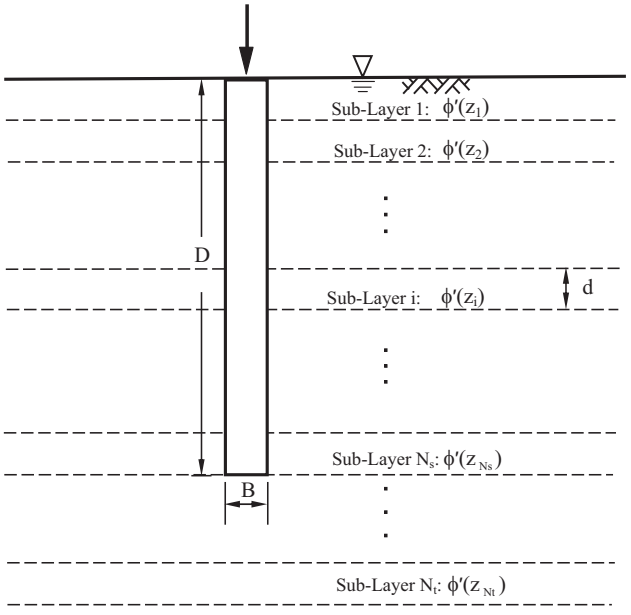

Fig. 1. Illustration of random field modeling.

into N_t sub-layers in RFM, and such sub-layers do not correspond to the soil layers identified based on the soil classification in geotechnical site investigation. The drilled shaft is installed in the upper N_s sub-layers, in which $N_s = D/d$. The ϕ' in each sub-layer is represented by an entry in the effective stress friction angle vector $\underline{\phi'} = [\phi'(z_1), \phi'(z_2), ..., \phi'(z_{Nt})]$, in which $\phi'(z_i)$ and z_i, $i=1, 2,..., N_t$, represent the effective stress friction angle ϕ' and average depth in the i-th sub-layer, respectively. In the context of a random field, the logarithm (i.e., $\underline{\ln \phi'} = [\ln \phi'(z_1), \ln \phi'(z_2), ..., \ln \phi'(z_{Nt})]$) of $\underline{\phi'}$ has the following representation (Wang et al., 2010a; Cao and Wang, 2013)

$$\underline{\ln \phi'} = \mu_{\ln \phi'}\underline{l} + \sigma_{\ln \phi'}\underline{L}^T\underline{x} \tag{2}$$

where $\mu_{\ln \phi'} = \ln \mu_{\phi'} - \sigma^2_{\ln \phi'}/2$ and $\sigma_{\ln \phi'} = \sqrt{\ln [1+(\sigma_{\phi'}/\mu_{\phi'})^2]}$ are the mean and standard deviation of the logarithm (i.e., $\ln \phi'$) of ϕ', respectively; $\underline{l}$= a vector with N_t components that are all equal to one; $\underline{x} = [x_1,..., x_{Nt}]^T = a$ standard Gaussian vector with N_t independent components; $\underline{L}$=a N_t-by-N_t upper-triangular matrix obtained by Cholesky decomposition of the correlation matrix $\underline{R}$ satisfying

$$\underline{R} = \underline{L}^T\underline{L} \tag{3}$$

and the (i,j)-th entry of $\underline{R}$ is given by the correlation function, e.g., Eq. (1).

Note that the random field is discretized into N_s sub-layers, and the soil property in each sub-layer is approximately represented by the random sample generated at the midpoint of the sub-layer in this study. Such an approximation is accurate only when the thickness (i.e., d) of the sub-layer is much smaller than the scale of fluctuation (i.e., λ) due to the effects of local spatial averaging (Vanmarcke, 1977). To ensure the accuracy of random field modeling, the thickness (i.e., d) of sub-layers needs to be very small with respect to the scale of fluctuation λ. In addition, a stationary (i.e., statistically homogeneous) random field is used herein to model the inherent spatial variability of soil properties (e.g., ϕ') in a soil layer, and the random field model parameters are considered spatially constant within the soil layer. However, it should be noted that soil properties (e.g., effective friction angle) might exhibit obvious spatial trends and, therefore, cannot be modeled directly using local stationary random fields. In such a case, the spatial trend needs to be removed (i.e., perform detrending or normalization) before using local stationary random fields to model the inherent spatial variability (e.g., Fenton, 1999a, b; Phoon et al., 2003; Cao and Wang, 2013).

Although the random field modeling (RFM) addresses the inherent spatial variability in a direct and explicit manner, research is relatively limited that applies RFM to model the inherent spatial variability of soil properties in the RBD of geotechnical structures. In current RBD approaches, the equivalent variance technique is commonly used to address the inherent spatial variability in an indirect and implicit manner. Effects of the indirect modeling method (i.e., equivalent variance technique) on RBD can be evaluated by comparing the design results when using RFM in RBD with those when using equivalent variance technique. For this purpose, this study also uses the equivalent variance technique to model, indirectly and implicitly, the inherent spatial variability in RBD of drilled shafts, as discussed in the next subsection.

2.2. Equivalent variance technique

In the equivalent variance technique, the soil property within a statistically homogenous soil mass (e.g., a depth interval Δz within a statistically homogenous soil layer) is characterized by a single random variable that represents the spatial average of the soil property over the soil mass and has a reduced variance due to the spatial averaging (e.g., Vanmarcke, 1977; Griffiths and Fenton, 2004; Luo et al., 2012). Consider, for example, the lognormally distributed ϕ' in a statistically homogenous soil layer where the drilled shaft is installed. Let $\phi'_{\Delta z}$ represents the spatial average of ϕ' over a depth interval Δz. Due to the spatial averaging over Δz, the variance of the equivalent normal random variable $\ln \phi'$ is reduced, and the variance reduction of $\ln \phi'$ is described by a variance reduction factor $\Gamma^2_{\Delta z}$ in the equivalent variance technique, which can be calculated as (e.g., Vanmarcke, 1977; Phoon and Kulhawy, 1999b; El-Ramly et al., 2002)

$$\Gamma^2_{\Delta z} = \begin{cases} 1 & \Delta z < \lambda \\ \lambda/\Delta z & \Delta z > \lambda \end{cases} \tag{4}$$

Eq. (4) gives a simplified form of the variance reduction function to conveniently calculate the variance reduction factor for various correlation structures, and it is valid for different correlation functions (Vanmarcke, 1977). Using Eq. (4) in the equivalent variance technique bypasses the need of determining the exact correlation structure of soil properties. It has been widely used in geotechnical literature (e.g., Vanmarcke, 1977; Phoon and Kulhawy, 1999b; El-Ramly et al., 2002). Therefore, Eq. (4) is applied in the equivalent variance technique to explore the effect of indirect modeling of inherent spatial variability on RBD of drilled shafts in this study.

For the drilled shaft design problem, the capacity of a drilled shaft consists of the side resistance $Q_{side}$and tip resistance Q_{tip}. Fig. 2 shows the respective influence zones for evaluating Q_{side} and Q_{tip}. The influence zone for evaluating Q_{side} is the depth interval along the shaft depth D, and, hence, its length is D. The influence zone for evaluating Q_{tip} includes a depth interval from L_a above the tip to L_b below the tip. The length (L) of influence zone for evaluating Q_{tip} is, therefore, equal to L_a+L_b, i.e., $L=L_a+L_b$. Calculations of Q_{side} and Q_{tip} need the values of ϕ' over their respective influence zones, i.e., the depth intervals of D and L. Let ϕ'_{side} and ϕ'_{tip} denote the respective spatial averages of ϕ' over D and L. ϕ'_{side} and ϕ'_{tip} can be written as (Griffiths and Fenton, 2004; Wang and Kulhawy, 2008)

$$\phi'_{side} = \exp(\mu_{\ln \phi'} + \sigma_{\ln \phi'}\sqrt{\Gamma^2_D}x_1) \tag{5}$$

$$\phi'_{tip} = \exp[\mu_{\ln \phi'} + \sigma_{\ln \phi'}\sqrt{\Gamma^2_L}(x_1\rho_A + x_2\sqrt{1-\rho^2_A})] \tag{6}$$

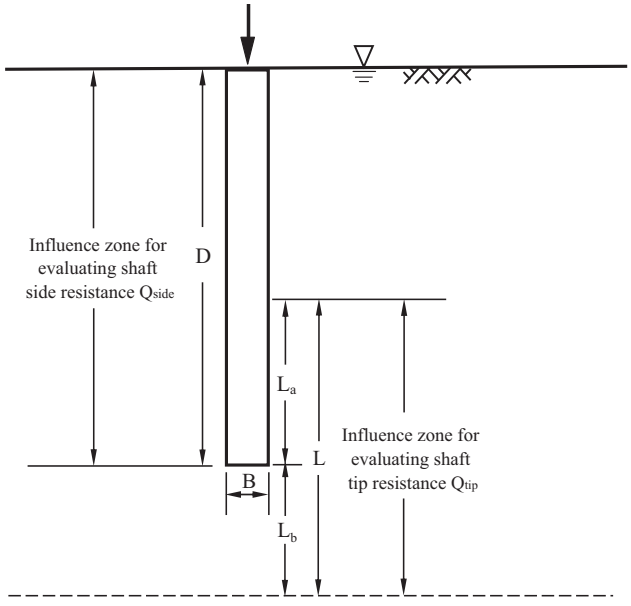

Fig. 2. Illustration of influence zones for evaluating the drilled shaft capacity.

in which x_1 and x_2= uncorrelated standard Gaussian random variables; Γ^2_D and Γ^2_L= the respective variance reduction factors of $\ln \phi'$ due to the spatial averaging over D and L, and they are calculated from Eq. (4) using their respective averaging intervals, i.e., $\Delta z = D$ for Γ^2_D and $\Delta z = L$ for Γ^2_L; ρ_A = the correlation coefficient between the logarithms (i.e., $\ln \phi'_{side}$ and $\ln \phi'_{tip}$) of ϕ'_{side} and ϕ'_{tip}, and it is given by (Vanmarcke, 1977, 1983; Zhang and Chen, 2012; Chen and Zhang, 2013)

$$\rho_A = \frac{D_0^2\Gamma^2_{D_0} - D_1^2\Gamma^2_{D_1} - D_2^2\Gamma^2_{D_2} + D_{12}^2\Gamma^2_{D_{12}}}{2DL\sqrt{\Gamma^2_D\Gamma^2_L}} \tag{7}$$

in which $D_0 = L_a$, $D_1 = D - L_a$, $D_2 = L_b$, and $D_{12} = D + L_b$; $\Gamma^2_{D_0}$, $\Gamma^2_{D_1}$, $\Gamma^2_{D_2}$, and $\Gamma^2_{D_{12}}$ = the respective variance reduction factors of $\ln \phi'$ due to the spatial averaging over the depth intervals D_0, D_1, D_2, and D_{12}, and they are calculated from Eq. (4) using their respective averaging intervals, i.e., D_0 for $\Gamma^2_{D_0}$, D_1 for $\Gamma^2_{D_1}$, D_2 for $\Gamma^2_{D_2}$, and D_{12} for $\Gamma^2_{D_{12}}$.

Note that the choice of influence zones for deterministic calculations of Q_{side} and Q_{tip} affects variance reduction factors (i.e., Γ^2_D, Γ^2_L, $\Gamma^2_{D_0}$, $\Gamma^2_{D_1}$, $\Gamma^2_{D_2}$, and $\Gamma^2_{D_{12}}$) in the equivalent variance technique. This subsequently influences the uncertainty modeling of ϕ' (see Eqs. (5) and (6)). When using the equivalent variance technique in RBD, the uncertainty modeling of ϕ' is, therefore, coupled with deterministic analysis of drilled shafts. In contrast, the RFM of inherent spatial variability can be deliberately decoupled from deterministic analysis of drilled shafts. This allows the deterministic analysis of drilled shafts and uncertainty modeling to be performed separately by personnel with different expertise and in a parallel fashion. This alleviates the geotechnical practitioners from reliability computational algorithm so that they can focus on the drilled shaft design problem itself. This will be further illustrated through a design example later. Both the RFM and equivalent variance technique are conveniently applied in the expanded RBD approach to model the inherent spatial variability of soil properties because the uncertainty modeling (e.g., inherent spatial variability modeling) is transparent to designers in the expanded RBD approach (Wang, 2011, 2013; Wang et al., 2011a). In the next section, the mathematical framework of the expanded RBD approach is introduced.

3. Expanded reliability-based design (expanded RBD) approach

The drilled shaft design process aims to find a set of B and D values that satisfy a series of pre-defined performance requirements, including the ultimate limit state (ULS) and serviceability limit state (SLS) requirements and the target failure probability p_T or target reliability index β_T. In the context of the expanded RBD approach, the drilled shaft design process is formulated as an expanded reliability problem (Au, 2005; Wang et al., 2011a), in which the design parameters (i.e., diameter B and depth D) are artificially considered as independent discrete random variables with uniformly distributed probability mass function $p(B,D)$. Then, the design process is revised as a process of calculating failure probabilities corresponding to designs with various combinations of B and D (i.e., conditional probability $p(\text{Failure}|B,D)$) and comparing them with p_T. Feasible designs are those with $p(\text{Failure}|B,D) \le p_T$. Failure herein refers to events in which the factor of safety (i.e., FS_{uls} or FS_{sls} for ULS or SLS requirements, respectively) is less than one. Using the Bayes' Theorem (e.g., Ang and Tang, 2007), the conditional probability $p(\text{Failure}|B,D)$ is given by

$$p(\text{Failure}|B,D) = \frac{p(B,D|\text{Failure})}{p(B,D)} p_f \tag{8}$$

in which $p(B,D|\text{Failure})$ = conditional joint probability of B and D given failure; p_f = the probability of failure; $p(B,D) = 1/(n_B n_D)$, where n_B and n_D are numbers of possible discrete values of B and D, respectively.

The expanded RBD approach employs a single run of direct MCS to estimate $p(B,D|\text{Failure})$ and p_f, which are further used in Eq. (8) to obtain $p(\text{Failure}|B,D)$ (Wang, 2011, 2013; Wang et al., 2011a). However, direct MCS suffers from a lack of efficiency and resolution at small probability levels, which are of great interest in design practice. This necessitates a large number of direct MCS samples for expanded RBD and requires extensive computational efforts, which might hamper the application of the approach in design practice. To improve the computational efficiency and generate failure samples efficiently for calculating $p(B,D|\text{Failure})$, p_f, and $p(\text{Failure}|B,D)$ in Eq. (8), the expanded RBD approach is enhanced with an advanced MCS called "Subset Simulation" (Au and Beck, 2001, 2003) in this study.

4. Subset Simulation

Subset Simulation is an advanced MCS method that uses conditional probability and Markov Chain Monte Carlo (MCMC) method to efficiently compute small tail probability (Au and Beck, 2001, 2003; Honjo, 2008). It expresses a rare event E with a small probability as a sequence of intermediate

events $\{E_1, E_2, \ldots, E_m\}$ with larger conditional probability and employs specially designed Markov chains to generate conditional samples of these intermediate events until the target sample domain is achieved. Let Y be the output parameter that is of interest and increases monotonically, and define the rare event E as $E=\{Y>y\}$, where y is a given threshold value for determining whether E occurs. In this study, Y is referred to as "driving variable". The choice of driving variable Y is pivotal to efficient generation of conditional samples of interest. For the drilled shaft design problem herein, Y is defined as BD/FS_{min}, in which FS_{min} is the minimum factor of safety (FS) among the FS_{uls} and FS_{sls} for respective ULS and SLS requirements. The selection of driving variable for the expanded RBD will be further discussed in a later section.

Let $y=y_m>y_{m-1}>\ldots>y_2>y_1>0$ be a decreasing sequence of intermediate threshold values. Then, the intermediate events $\{E_k,\ k=1,\ 2,\ \ldots,\ m\}$ are defined as $E_k=\{Y>y_k\}$, $k=1, 2, \ldots, m$. By sequentially conditioning on the intermediate events $\{E_k,\ k=1,\ 2,\ \ldots,\ m\}$, the probability of event E, i.e., $p(E=\{Y>y\})$, can be written as

$$p(E)=p(E_m)=p(E_1)\prod_{k=2}^{m}p(E_k|E_{k-1}) \tag{9}$$

in which $p(E_1)$=probability of E_1; $p(E_k|E_{k-1})$=probability of E_k conditional on E_{k-1}. In implementations, $y_1, y_2, \ldots y_m$ are generated adaptively using information from simulated samples so that the sample estimate of $p(E_1)$ and $\{p(E_k|E_{k-1}),\ k=2, \ldots, m\}$ always corresponds to a common specified value of conditional probability p_0.

Subset Simulation has been applied to geotechnical engineering problems (e.g., Santoso et al., 2009; Au et al., 2010; Wang et al., 2010b, 2011b). It has recently been programmed in a commonly-available EXCEL spreadsheet environment as a VBA Add-In and can be readily used by practitioners (Au et al., 2010). Further details of Subset Simulation and its implementation in the EXCEL spreadsheet environment are referred to Au and Beck (2001 and 2003), Au et al. (2010), and Wang et al., (2010b).

5. Integration of expanded RBD approach with Subset Simulation

Consider designing a drilled shaft by the expanded RBD approach and performing a Subset Simulation with $m+1$ levels of simulations to estimate $p(B,D|\text{Failure})$, p_f, and $p(\text{Failure}|B,D)$ in Eq. (8). In the expanded RBD approach, B and D are artificially treated as uncertain parameters, and their random samples are generated in Subset Simulation. The sample space Ω of B and D is divided into $m+1$ individual subsets $\{\Omega_k,\ k=0, 1, 2, \ldots, m\}$ by the intermediate threshold values $\{y_k,\ k=1, 2, \ldots, m\}$ of $Y=\text{BD}/FS_{min}$, in which Ω_0 is the complementary set of E_1 (i.e., $\Omega_0=\{0\le Y\le y_1\}$); $\Omega_k,\ k=1, \ldots, m-1$ is equal to E_k–E_{k+1} (i.e., $\Omega_k=\{y_k<Y\le y_{k+1}\}$); and Ω_m is equal to E_m (i.e., $\Omega_m=\{Y>y_m\}$). In Subset Simulation, the intermediate threshold values $\{y_k,\ k=1, 2, \ldots, m\}$ are adaptively determined to generate m+1 individual subsets $\{\Omega_k,\ k=0, 1, 2, \ldots, m\}$ of B and D, and samples in different subsets are generated level by level and carry different weights in the calculation of p_f and $p(B,D|\text{Failure})$. According to the Theorem of Total Probability (e.g., Ang and Tang, 2007), p_f is expressed as

$$p_f=\sum_{k=0}^{m}p(\text{Failure}|\Omega_k)p(\Omega_k) \tag{10}$$

where $p(\text{Failure}|\Omega_k)$=the conditional failure probability given sampling in Ω_k; $p(\Omega_k)$=the probability of the event Ω_k. $p(\text{Failure}|\Omega_k)$ is estimated as the ratio of the failure sample number in Ω_k over the total sample number in Ω_k. $p(\Omega_k)$ is calculated as

$$\begin{aligned}&p(\Omega_0)=1-p_0\\&p(\Omega_k)=p_0^k-p_0^{k+1},\quad k=1,\ \ldots m-1\\&p(\Omega_m)=p_0^m\end{aligned} \tag{11}$$

Note that $\Omega_k,\ k=0, 1, 2, \ldots, m$, are mutually exclusive and collectively exhaustive events, i.e., $p(\Omega_k\cap\Omega_j)=0$ for $k\ne j$ and $\sum_{k=0}^{m}p(\Omega_k)=1$. When $p(\text{Failure}|\Omega_k)$, $p(\Omega_k)$, and p_f are obtained, the conditional probability $p(\Omega_k|\text{Failure})$ is calculated using the Bayes' Theorem

$$p(\Omega_k|\text{Failure})=\frac{p(\text{Failure}|\Omega_k)p(\Omega_k)}{p_f} \tag{12}$$

Then, the conditional probability $p(B,D|\text{Failure})$ of a specific combination of B and D is given by the Theorem of Total Probability as

$$p(B,D|\text{Failure})=\sum_{k=0}^{m}p(B,D|\text{Failure}\cap\Omega_k)p(\Omega_k|\text{Failure}) \tag{13}$$

where $p(B,D|\text{Failure}\cap\Omega_k)$=the conditional probability of a combination of B and D given sampling in Ω_k and occurrence of failure, and it is expressed as the ratio of the number of failure samples in Ω_k with a combination of B and D over the total failure sample number in Ω_k. Let $n_{\Omega k}$ denote the total failure sample number in Ω_k. Among these $n_{\Omega k}$ failure samples in Ω_k, there might exist various combinations of B and D. If the number of failure samples for a given combination of B and D in Ω_k is denoted as $n_{\Omega k,BD}$. Then, the $p(B,D|\text{Failure}\cap\Omega_k)$ value for the given combination of B and D is calculated as $n_{\Omega k,BD}/n_{\Omega k}$.

Using Eq. (10)–(13), p_f and $p(B,D|\text{Failure})$ are calculated from the Subset Simulation. Then, $p(\text{Failure}|B,D)$ is given by Eq. (8). Since failure is defined as $FS_{uls}<1$ for ULS or $FS_{sls}<1$ for SLS, two sets of conditional failure probabilities $p(\text{Failure}|B,D)$ [i.e., the conditional ULS and SLS failure probabilities (p_f^{ULS} and p_f^{SLS}) given different combinations of B and D] are calculated for the drilled shaft design. Finally, feasible design values of B and D are determined by comparing the $p(\text{Failure}|B,D)$ with p_T. To facilitate the design practice, this study implements Eqs. (8) and (10)–(13) in a commonly-available EXCEL spreadsheet environment as a VBA Add-In to calculate the conditional failure probability (e.g., $p(\text{Failure}|B,D)$) for expanded RBD, and combines the RBD Add-In and the Subset Simulation Add-In developed by Au et al. (2010)

together. The combined Add-In is further illustrated in the next section.

6. Illustrative example

Phoon et al. (1995) illustrated the multiple resistance factor design (MRFD) approach using a drilled shaft design example shown in Fig. 3. This drilled shaft is installed in loose sand with a total unit weight $\gamma=20.0$ kN/m^3, mean effective stress friction angle $\mu_{\phi'}=32^\circ$, and mean at-rest coefficient of horizontal soil stress $\mu_{K_0}=1.0$. The shaft diameter B, concrete unit weight γ_{con}, and nominal operative in-situ horizontal stress coefficient ratio $(K/K_0)_n$ are 1.2 m, 24.0 kN/m^3, and 1.0, respectively, and the water table is at the ground surface. The shaft is assumed to fail in drained general shear under a design compression load $F_{50}=800$ kN with an allowable displacement $y_a=25$ mm. The key design parameters in this example are the drilled shaft diameter B and depth D, which are required to support the design compression load without ULS failure and to have a shaft displacement less than 25 mm. Using the MRFD approach, Phoon et al. (1995) showed that $D=5.0$ m is a feasible design for ULS and SLS p_T of $p_T^{ULS}=0.00069$ (i.e., $\beta_T^{ULS}=3.2$) and $p_T^{SLS}=0.0047$ (i.e., $\beta_T^{SLS}=2.6$) when COV$_{\phi'}=15\%$–20% and $B=1.2$ m. Note that Phoon et al. (1995) models ϕ' in the sand layer by a single random variable. The inherent spatial variability of ϕ' in the sand layer is, therefore, not modeled directly or explicitly in their study.

To account directly and explicitly for the inherent spatial variability of ϕ' in RBD, the proposed approach is used to re-design the drilled shaft design example in this section. The proposed approach is implemented in a commonly-available EXCEL spreadsheet environment by a package of worksheets and VBA functions/Add-Ins. The implementation is divided into three parts: deterministic model worksheet, uncertainty model worksheet, and Subset Simulation and RBD Add-In. The uncertainty modeling and propagation by Subset Simulation and calculation of the conditional failure probability for the expanded RBD are deliberately decoupled from the deterministic model worksheet for traditional drilled shaft design calculation so they can proceed as an extension of the deterministic calculation in a non-intrusive manner. Details of the three parts of modeling are introduced in the following three subsections, respectively.

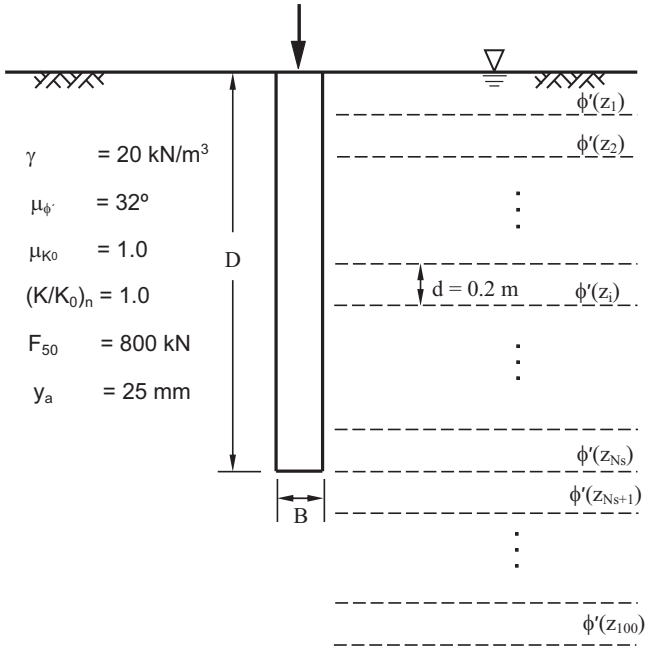

Fig. 3. Design example of drilled shaft under drained compression. Modified from Phoon et al. (1995) and Wang et al. (2011a).

6.1. Deterministic model worksheet

The deterministic model is largely identical to the traditional drilled shaft design calculation. It takes a given set of system parameters (e.g., design parameters B and D, design loads, and soil properties) as input and provides the values of FS$_{uls}$, FS$_{sls}$, and BD/FS$_{min}$ corresponding to the set of system parameters as output. As defined by Phoon et al. (1995), the drilled shaft has a design load $F_{50}=800$ kN and an allowable displacement $y_a=25$ mm. As shown in Fig. 3, the sand layer surrounding the drilled shaft is divided into 100 0.2 m-thick sub-layers (i.e., $N_t=100$ in this example) and the drilled shaft is installed in the upper N_s sub-layers, where $N_s=$D/0.2. The FS$_{uls}$ and FS$_{sls}$ of the drilled shaft are calculated from

$$\mathrm{FS}_{uls}=Q_{uls}/F_{50}=(Q_{side}+Q_{tip}-W)/F_{50} \tag{14}$$

$$\mathrm{FS}_{sls}=Q_{sls}/F_{50}=0.625a\left(\frac{y_a}{B}\right)^b Q_{uls}/F_{50} \tag{15}$$

where Q_{uls} and $Q_{sls}=$ULS and SLS capacity, respectively; Q_{side}, Q_{tip}, and $W=$side resistance, tip resistance, and effective shaft weight, respectively; and $a=4.0$ and $b=0.4$ are curve-fitted parameters for the load–displacement model. The Q_{side}, Q_{tip}, and W are calculated from

$$Q_{side}=\sum_{i=1}^{Ns} Q_{side,i}=\pi Bd(K/K_0)_n K_0\left[\sum_{i=1}^{Ns}(\sigma'_{v,i}\ \tan\ \delta_i)\right] \tag{16}$$

$$Q_{tip}=0.25\pi B^2[0.5B(\gamma-\gamma_w)N_\gamma\zeta_{\gamma s}\zeta_{\gamma d}\zeta_{\gamma r}+D(\gamma-\gamma_w)N_q\zeta_{qs}\zeta_{qd}\zeta_{qr}] \tag{17}$$

$$W=0.25\pi B^2D(\gamma_{con}-\gamma_w) \tag{18}$$

in which $Q_{side,i}=$the side resistance provided by the i-th sub-layer; $\sigma'_{v,i}=$ the average vertical effective stress in the i-th sub-layer; $\delta_i=$ the friction angle at the soil-shaft interface in the i-th sub-layer$=$ the effective stress friction angle $\phi'(z_i)$ in the i-th sub-layer (for a rough interface); $K_0=$at-rest coefficient of horizontal soil stress$=1.0$ in this example; $d=$the sub-layer thickness$=0.2$ m in this study; $\gamma_w=$unit weight of water; $N_q=[\tan^2(45^\circ+\overline{\phi'}/2)]\exp(\pi\tan\overline{\phi'})$ and $N_\gamma=2(N_q+1)\tan\overline{\phi'}$ are bearing capacity factors, where $\overline{\phi'}=$average value of ϕ' within the influence zone for evaluating the tip resistance$=(d/L)\sum_{i=(Ns-L_a/d+1)}^{(Ns+L_b/d)}\phi'(z_i)$; $\zeta_{\gamma s}=0.6$, $\zeta_{\gamma d}=\zeta_{\gamma r}=1$, $\zeta_{qs}=1+\tan\overline{\phi'}$, $\zeta_{qd}=1+2\tan\overline{\phi'}(1-\sin\overline{\phi'})^2[(\pi/180)\tan^{-1}(D/B)]$, and $\zeta_{qr}=1$ are correction factors for respective bearing capacity factors. The bearing

capacity and correction factors are calculated using the basic Vesić (1975) model with minor updates (Kulhawy, 1991). Determining the bearing capacity and correction factors requires the average value (i.e., $\overline{\phi'}$) of ϕ' within the influence zone for evaluating Q_{tip}. In this study, the influence zone for evaluating Q_{tip} is taken as the depth interval from 8B above the shaft tip to 3.5B below the shaft tip, i.e., $L_a=8B$ and $L_b=3.5B$ (Schmertmann, 1967; Zhang and Chen, 2012). When $8B > D$, L_a is taken as D, i.e., $L_a=\min\{8B,D\}$, where min{ } denotes the minimum among $8B$ and D. After Q_{side}, Q_{tip}, and W are obtained, FS_{uls} and FS_{sls} are calculated from Eqs. (14) and (15), respectively, and BD/FS_{min} is also calculated in the deterministic model worksheet. Failure occurs when $FS_{uls} \le 1$ or $FS_{sls} \le 1$. In addition, it is worthwhile to point out that although the FS_{uls} and FS_{sls} are calculated using Eqs. (14)–(18) in this example, the proposed approach allows general choices of the deterministic model, including empirical bearing capacity equations, for calculating the FS_{uls} and FS_{sls} of drilled shafts. However, the use of such an empirical bearing capacity equation has to follow the way the soil parameter value was treated in the development of the equation. For example, average soil parameter values (e.g., the average value of ϕ' within the influence zone for evaluating the tip resistance) should be used in this example.

Fig. 4 shows the deterministic model worksheet in EXCEL spreadsheet. The worksheet is divided into three parts: an input zone, a capacity calculation zone, and an output zone. The input zone contains the input information required for calculating the capacity of the drilled shaft, such as soil properties, design parameters, etc. The input information is used to calculate Q_{side}, Q_{tip}, W, Q_{uls} and Q_{sls} in the capacity calculation zone. Then, FS_{uls} and FS_{sls} are calculated in the output zone using Eqs. (14) and (15), and the driving variable BD/FS_{min} is also calculated in the output zone. From an input–output perspective, the deterministic model worksheet takes a given set of values of system parameters as input, calculates the safety factors and driving variable, and returns the driving variable as an output. No probability concept is involved in the deterministic model worksheet, and it can be developed by practitioners without a probabilistic analysis background.

6.2. Uncertainty model worksheet

An uncertainty model worksheet is developed to define the uncertain system parameters that are treated as random variables in the expanded RBD approach and to generate random samples of the random variables using their respective statistics and distribution types. To account directly and explicitly for the inherent spatial variability of ϕ', this section models ϕ' in the sand layer by a one-dimensional lognormal random field $\underline{\phi'} = [\phi'(z_1), \phi'(z_2), ..., \phi'(z_{100})]$, as shown in Fig. 3. $\mu_{\phi'}$ and $\sigma_{\phi'}$ of ϕ' are taken as 32° and 5.44° (i.e., $COV_{\phi'}=17\%$), respectively, which are consistent with those values adopted by Phoon et al. (1995). The correlation structure is given by Eq. (1), and λ is taken as 4 m, which falls within the typical range of the vertical scale of fluctuation of in-situ test data on strength parameters of soil reported in the geotechnical literature, e.g., from 2 m to 6 m (Phoon and Kulhawy, 1999a,b). In addition, since B and D are artificially treated as uniformly distributed random variables in the expanded RBD approach, their random samples are also generated in the uncertainty model worksheet during simulation. In this study, three possible B values of 0.9 m, 1.2 m, and 1.5 m (i.e., $n_B=3$) are considered, and the possible D values vary from 2.0 m to 10.0 m with an increment of 0.2 m (i.e., $n_D=41$).

Fig. 5 shows the uncertainty model worksheet, which consists of three parts: a variable description zone, a random sample generation zone, and a zone that contains the lower-triangular matrix (i.e., $\underline{L}^T$ in Eq. (2)) obtained from Cholesky decomposition of the correlation matrix $\underline{R}$. The variable description zone contains the information on distribution types

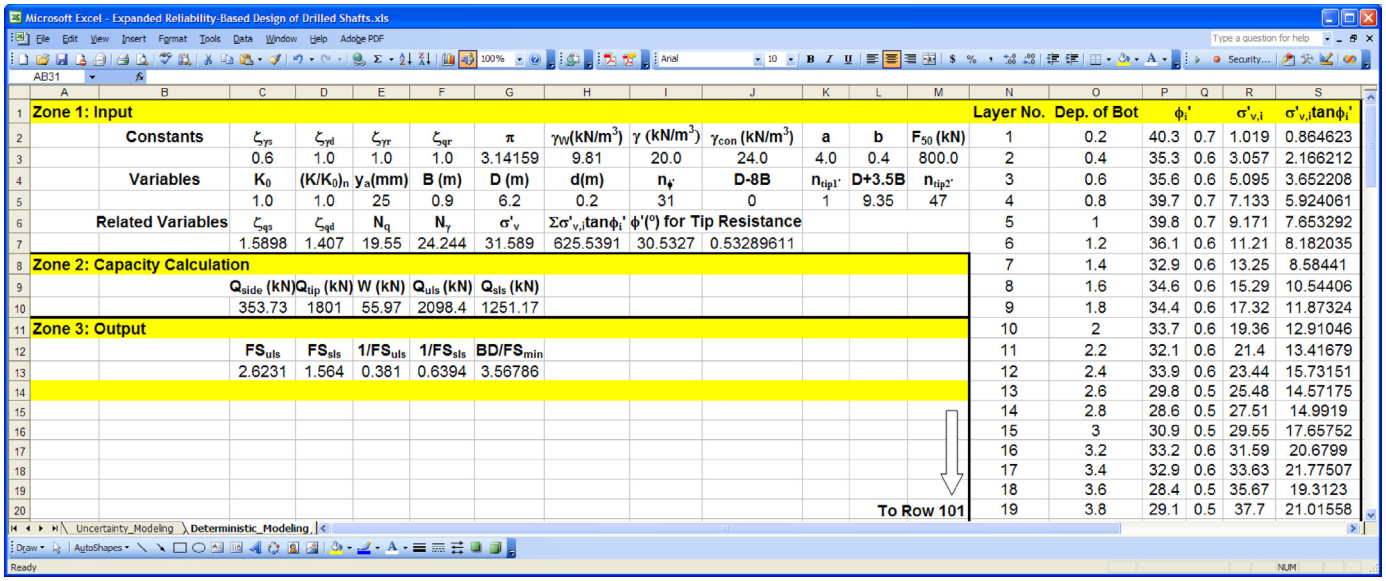

Fig. 4. Deterministic model worksheet.

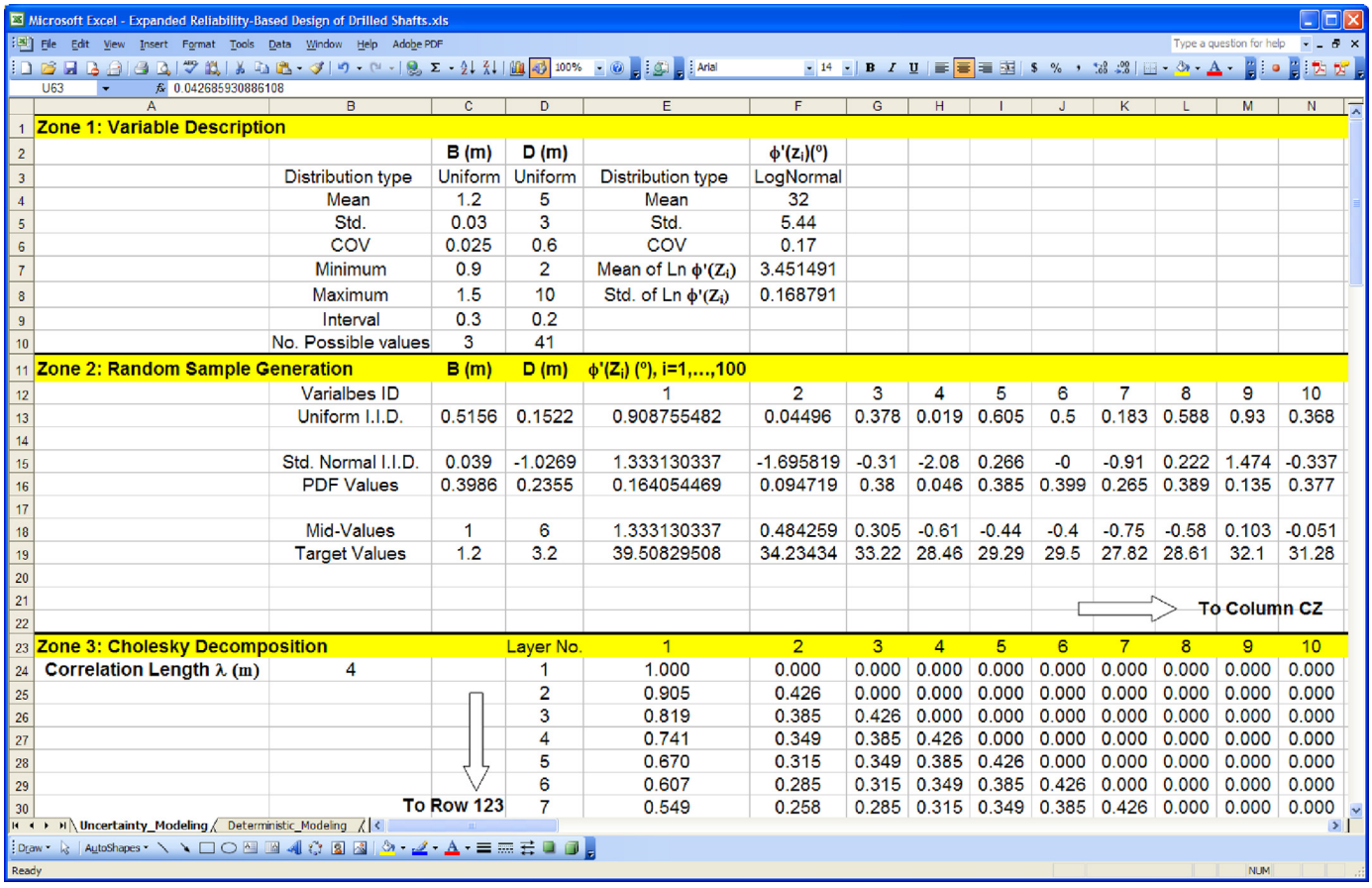

Fig. 5. Uncertainty model worksheet.

and statistics of random variables $\phi'(z_i)$, $i=1, 2, \ldots,100$, B, and D. Such information is used to generate random samples of $\phi'(z_i)$, B, and D in the random sample generation zone. The generation of random samples starts with generating uniform random samples using an EXCEL built-in function "RAND()", which are then transformed to random samples of the target distribution types (e.g., discrete uniform distributions of B and D and lognormal distribution of $\phi'(z_i)$). In this study, the correlated random samples of $\phi'(z_i)$, $i=1, 2, \ldots,100$, are generated using Eq. (2), in which $\underline{L}^T$ is given by the zone starting from Row 23 (see Fig. 5). Details of the random sample generation process in EXCEL are referred to Au et al. (2010). From an input–output perspective, the uncertainty model worksheet takes no input but returns a set of random samples of the uncertain system parameters as its output. It can be developed in parallel with the deterministic model worksheet.

When the deterministic model worksheet and uncertainty model worksheet are developed, they are linked together through their input/output cells to execute a reliability analysis of the drilled shaft. The link is carried out by simply setting the cell references for nominal values of uncertain parameters in deterministic model worksheet to be the cell references for the random samples in the uncertainty model worksheet. After this task, the values of uncertain system parameters shown in the deterministic model worksheet are equal to those generated in the uncertainty model worksheet, so the values of FS_{uls}, FS_{sls}, and BD/FS_{min} calculated in the deterministic model worksheet are random.

6.3. Subset Simulation and RBD Add-In

When the deterministic model worksheet and uncertainty model worksheet are completed and linked together, the Subset Simulation and RBD Add-In developed in this study is invoked for uncertainty propagation and calculating the conditional failure probability (i.e., $p(\text{Failure}|B,D)$ in this study) for expanded RBD. Fig. 6 shows the Subset Simulation and RBD Add-In developed in this study, which consists of two userform pages: one for implementing Subset Simulation and the other for calculating conditional failure probability for expanded RBD using random samples generated in Subset Simulation according to Eqs. (8) and (10)–(13).

Fig. 6(a) shows the userform page for implementing Subset Simulation. There are eight input fields on the Subset Simulation userform page. They are used to specify the number of Subset Simulation runs, number of samples per level N, conditional probability from one level to next p_0, the highest Subset Simulation level m, cell references of the random variables and their PDF values, and cell references of the driving variable (e.g., $Y=BD/FS_{min}$) and other variables V (e.g., random samples and their corresponding $1/FS_{uls}$ and

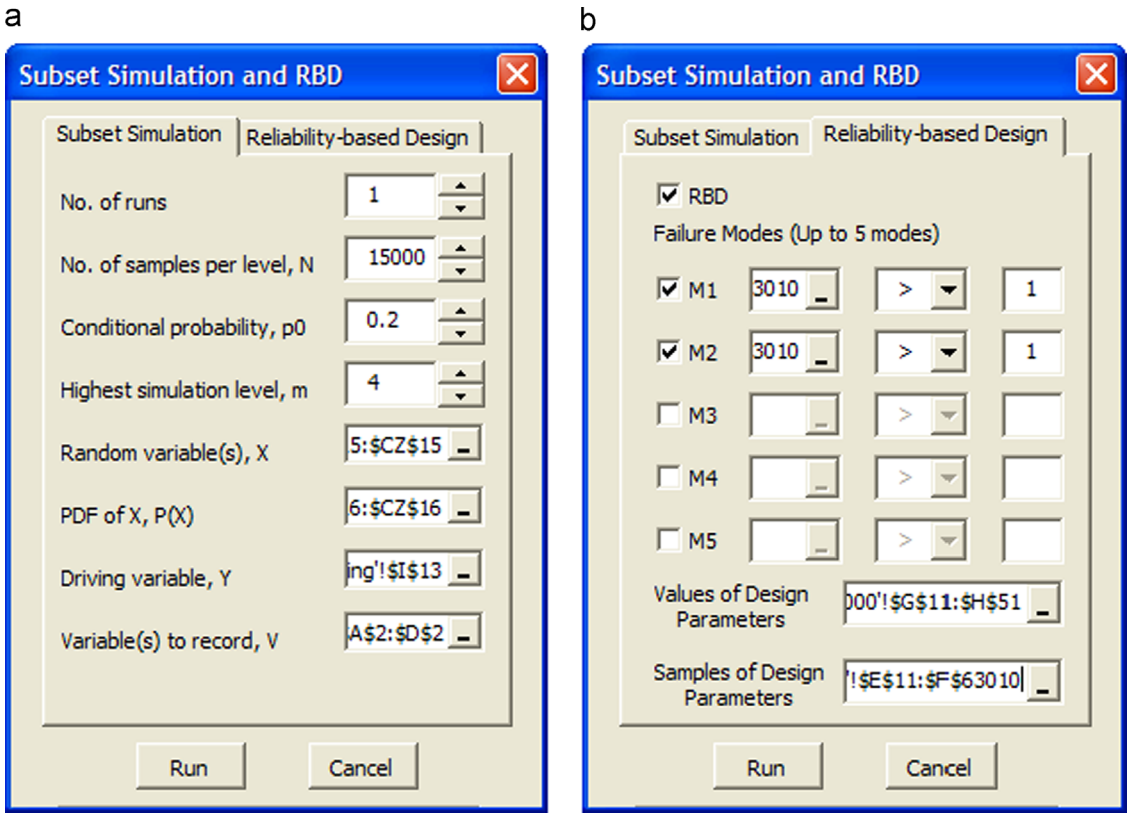

Fig. 6. Subset Simulation and RBD Add-In. (a) Subset Simulation userform page and (b) reliability-based design userform page.

$1/FS_{sls}$) of interest, respectively. After setting up the userform page, Subset Simulation starts by clicking the "Run" button. Using the Add-In, a Subset Simulation run with $N=15{,}000$, $p_0=0.2$, and $m=4$ is executed, in which a total of $N+mN(1-p_0)=63{,}000$ samples (Au et al., 2010) are simulated. After the simulation, an output worksheet is created by the Add-In to record the simulation results, including the random samples generated in simulation and their corresponding values of $1/FS_{uls}$, $1/FS_{sls}$, and BD/FS_{min}. The simulation results are used as input of the RBD userform page to calculate $p(\text{Failure}|B,D)$ for ULS and SLS failures.

Fig. 6(b) shows the RBD userform page of the Add-In. The checkbox "RBD" at the top of the userform page is used to enable/disenable the input fields of "Failure Modes", "Values of Design Parameters", and "Samples of Design Parameters" for RBD. The Add-In is able to calculate, simultaneously, conditional failure probability for five failure modes, e.g., ULS and SLS failures in this study. Each failure mode is defined by three input fields, including the system response (e.g., values of $1/FS_{uls}$ or $1/FS_{sls}$ of random samples generated during Subset Simulation) of interest, the type of the failure criterion (i.e., $>$, $=$, or $<$), and a critical value (e.g., one for $1/FS_{uls}$ and $1/FS_{sls}$) for judging the failure occurrence. The two input fields (i.e., "Values of Design Parameters" and "Samples of Design Parameters") in the bottom require cell references of possible values of design parameters (e.g., B and D in this study) and their random samples generated during Subset Simulation, respectively. After setting up the userform page, calculating the conditional failure probability starts by clicking the "Run" button. After the calculation, the RBD Add-In provides a result worksheet for each failure mode, which contains the conditional failure probability of designs with various combinations of design parameters for the failure mode and a plot of the conditional failure probability versus design parameters, e.g., Fig. 7(a) and (b) for ULS and SLS failures, respectively.

6.4. Determination of feasible designs

Fig. 7 shows the values of $p(\text{Failure}|B,D)$ (i.e., p_f^{ULS} and p_f^{SLS} for ULS and SLS failures, respectively) obtained from a single run of Subset Simulation by solid lines. The $p(\text{Failure}|B,D)$ is a variation of failure probability as a function of (B,D). The horizontal axis in Fig. 7 represents the variation of D, and the values of p_f^{ULS} or p_f^{SLS} for three different values of B are included in the figure. For a given value of B, both p_f^{ULS} and p_f^{SLS} decrease as D increases. Similarly, for a given value of D, both p_f^{ULS} and p_f^{SLS} decrease as B increases. Fig. 7 also includes the $p_T^{ULS}=0.00069$ and $p_T^{SLS}=0.0047$ adopted by Phoon et al. (1995), and feasible designs are those that fall below the p_T^{ULS} and p_T^{SLS} shown in the figure.

For the ULS requirement, the feasible designs include the drilled shafts with $B=1.5$ m and $D\geq 2.6$ m, $B=1.2$ m and $D\geq 3.8$ m, or $B=0.9$ m and $D\geq 5.6$ m (see Fig. 7(a)). For the SLS requirement, the feasible designs include those with $B=1.5$ m and $D\geq 4.0$ m, $B=1.2$ m and $D\geq 5.2$ m, or $B=0.9$ m and $D\geq 7.2$ m (see Fig. 7(b)). For a given value of B, the minimum feasible values (i.e., 4.0 m, 5.2 m, and 7.2 m for $B=1.5$ m, 1.2 m and 0.9 m, respectively) of D for the SLS

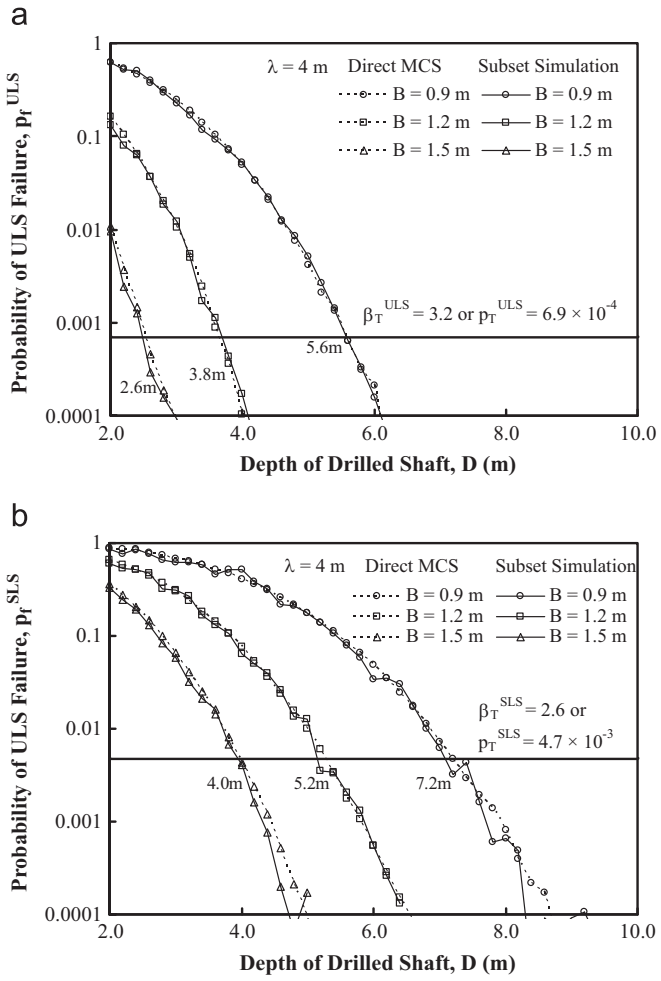

Fig. 7. Conditional failure probability obtained from Subset Simulation and direct MCS. (a) Ultimate limit state (ULS) failure and (b) serviceability limit state (SLS) failure.

requirement are larger than those (i.e., 2.6 m, 3.8 m, and 5.6 m for $B=1.5$ m, 1.2 m and 0.9 m, respectively) for the ULS requirement. The SLS requirement is therefore the critical one that controls the design, and the feasible designs are the same as those for the SLS requirement. Phoon et al. (1995) also found that the SLS requirement is the critical one in this design example, which is consistent with the observation herein.

6.5. Validation of Subset Simulation results

To validate the results obtained from Subset Simulation, the values of p_f^{ULS} and p_f^{SLS} for various combinations of B and D are also re-evaluated by the expanded RBD approach with direct MCS. A single run of direct MCS with 20,000,000 samples is performed to calculate the values of p_f^{ULS} and p_f^{SLS} in this example. To enable a consistent comparison with the results obtained from Subset Simulation, the deterministic modeling for calculating FS_{uls} and FS_{sls} and uncertainty modeling for generating random samples in direct MCS follow those adopted in Subset Simulation. Details of the expanded RBD approach with direct MCS are referred to Wang (2011), Wang et al. (2011a), and Wang (2013).

Fig. 7 also includes the results of p_f^{ULS} and p_f^{SLS} obtained from a single run of direct MCS by dashed lines. For a given value of B, the dashed line plots closely to the solid line. The results obtained from direct MCS are in good agreement with those obtained from Subset Simulation. Such agreement validates the proposed expanded RBD approach with Subset Simulation. Compared with the expanded RBD approach with direct MCS, only 63,000 random samples are, however, generated in Subset Simulation, which are much less than the 20,000,000 samples used in direct MCS. Subset Simulation improves, significantly, the computational efficiency at small probability levels, and it significantly enhances the expanded RBD approach in design situations with a small target failure probability (e.g., $p_T^{ULS}=0.00069$ and $p_T^{SLS}=0.0047$ in this study).

7. Effects of scale of fluctuation

The proposed approach accounts, directly and explicitly, for inherent spatial variability of soil properties in RBD through RFM. In the RFM, the spatial correlation is characterized by the scale of fluctuation λ and the correlation structure. A sensitivity study is carried out in this section to explore the effect of the scale of fluctuation on RBD of drilled shafts together with the single exponential correlation structure (i.e., Eq. (1)). In addition, the effect of the correlation structure is explored in the next section.

For consideration of different spatial correlations, a series of Subset Simulation runs are performed with different λ values varying from 0.5 m to $+\infty$, each of which has $m=4$, $p_0=0.2$, and $N=15,000$. As implied by Eq. (1), the spatial correlation increases as λ increases for a given separation distance $|z_i-z_j|$. When $\lambda=+\infty$, the components in $\underline{\phi'}$ are fully correlated and the spatial variability is ignored [i.e., $\phi'(z_1)=\phi'(z_2)=,...,=\phi'(z_{100})$]. After each Subset Simulation run, the values of p_f^{ULS} and p_f^{SLS} for different combinations of B and D are calculated using the RBD Add-In (see Fig. 6(b)), and the feasible designs for the λ value used in the Subset Simulation run are then determined accordingly by comparing the values of p_f^{ULS} and p_f^{SLS} with $p_T^{ULS}=0.00069$ and $p_T^{SLS}=0.0047$, respectively.

Fig. 8 shows the variation of the minimum feasible value (i.e., D_{min}) of D for $B=0.9$ m, 1.2 m, and 1.5 m as a function of the scale of fluctuation λ by three solid lines with circles, squares, and triangles, respectively. The three solid lines follow a similar trend. As λ increases from 0.5 m to $+\infty$, D_{min} increases from 5.4 m to 10.0 m, from 3.6 m to 8.0 m, and from 2.6 m to 6.2 m for B = 0.9 m, 1.2 m and 1.5 m, respectively. The scale of fluctuation affects the RBD of the drilled shaft significantly. If soil properties (e.g., ϕ') are considered fully correlated or the inherent spatial variability is ignored (i.e., $\lambda=+\infty$), D_{min} is over-estimated significantly and the design is conservative, particularly when the spatial variability is relatively significant (i.e., λ is relatively small). This is attributed to the over-estimation of the failure probability of the designs at small probability levels when ignoring inherent spatial variability (e.g., Sivakumar Babu and Mukesh, 2004; Griffiths and Fenton, 2004; Wang et al., 2011b). The proposed approach in

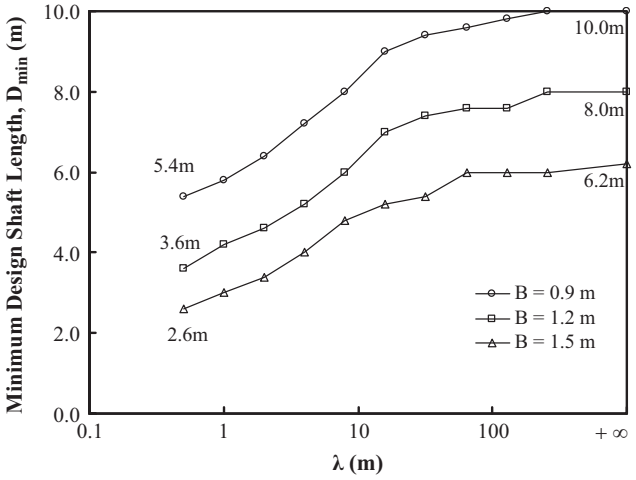

Fig. 8. Effects of scale of fluctuation on feasible designs.

this study accounts for the effect of the scale of fluctuation on RBD of drilled shafts in a direct and explicit manner.

8. Effects of correlation structure

To explore the effect of the correlation structure on RBD of drilled shafts, the design example shown in Fig. 3 is re-designed using the proposed approach together with a correlation structure different from Eq. (1) in the RFM. Consider, for example, a cosine exponential correlation function (e.g., Vanmarcke, 1977; Phoon et al., 2003)

$$\rho_{ij} = \exp(-|z_i - z_j|/\lambda)\cos\,[(z_i - z_j)/\lambda] \tag{19}$$

A Subset Simulation run with m=4, p_0=0.2, and N=15,000 is then performed to re-evaluate the values of p_f^{ULS} and p_f^{SLS} for various combinations of B and D, in which the inherent spatial variability is modeled by the RFM together with Eq. (19) and λ=4 m. To enable a consistent comparison with the results obtained using Eq. (1), the uncertainty modeling and deterministic modeling in the Subset Simulation generally follow those adopted in the illustrative example (see the Subsections entitled "Uncertainty Model Worksheet" and "Deterministic Model Worksheet", respectively), except for the correlation structure.

Fig. 9 shows the values of p_f^{ULS} and p_f^{SLS} for the designs with various combinations of B and D obtained using the cosine exponential correlation structure by dashed lines. For comparison, Fig. 9 also includes the results of p_f^{ULS} and p_f^{SLS} obtained using the single exponential correlation structure and λ=4 m by solid lines. For a given value of B, the dashed line generally plots above the solid line. Compared with the results obtained using the single exponential correlation function, using the cosine exponential correlation function in the RFM leads to relatively large values of p_f^{ULS} and p_f^{SLS} for a given design at small probability levels. This subsequently results in relatively conservative feasible designs at the target failure probability level (e.g., p_T^{ULS}=0.00069 and p_T^{SLS}=0.0047, see Fig. 9). The correlation structure has considerable effects on RBD of drilled shafts. Such effects are considered, directly and explicitly, in RBD using the proposed approach.

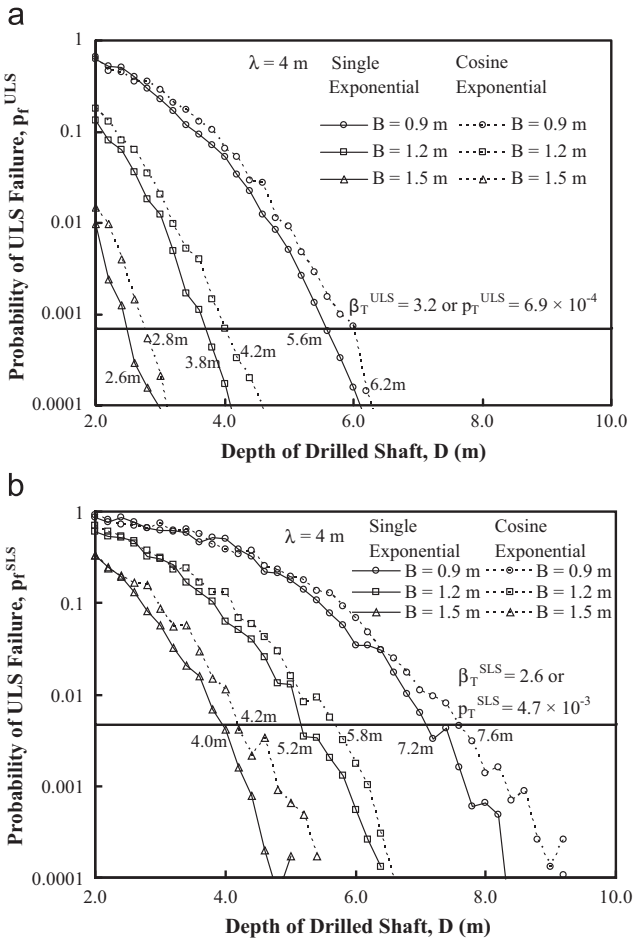

Fig. 9. Conditional failure probability obtained using different correlation structures. (a) Ultimate limit state (ULS) failure and (b) serviceability limit state (SLS) failure.

9. Effects of the indirect modeling method

To evaluate the effect of the indirect modeling of inherent spatial variability using the equivalent variance technique in RBD of drilled shafts, this section applies the expanded RBD approach with Subset Simulation to re-design the drilled shaft design example together with the equivalent variance technique to model the inherent spatial variability of ϕ'. As discussed in the Subsection entitled "Equivalent Variance Technique", ϕ' in the soil layer surrounding the drilled shaft is modeled by ϕ'_{side} and ϕ'_{tip} in the equivalent variance technique, which represent the respective spatial averages of ϕ' over the shaft depth D and the length L (e.g., $\min\{8B,D\}+3.5B$ in this study) of the influence zone for evaluating Q_{tip}. Using Eqs. (5) and (6), the random samples of ϕ'_{side} and ϕ'_{tip} are generated in the uncertainty model worksheet, respectively. In addition, the random samples of B and D are also simulated in the uncertainty model worksheet.

For each set of random samples, Q_{tip} is calculated from Eq. (17) using $\overline{\phi'} = \phi'_{tip}$, and Q_{side} is given by

$$Q_{side} = \pi BD(K/K_0)_n K_0 \sigma'_v \tan\,\phi'_{side} \tag{20}$$

where σ'_v = mean effective stress along the shaft depth. In addition, effective shaft weight W is obtained from Eq. (18). Then, the FS_{uls} and FS_{sls} are given by Eqs. (14) and (15),

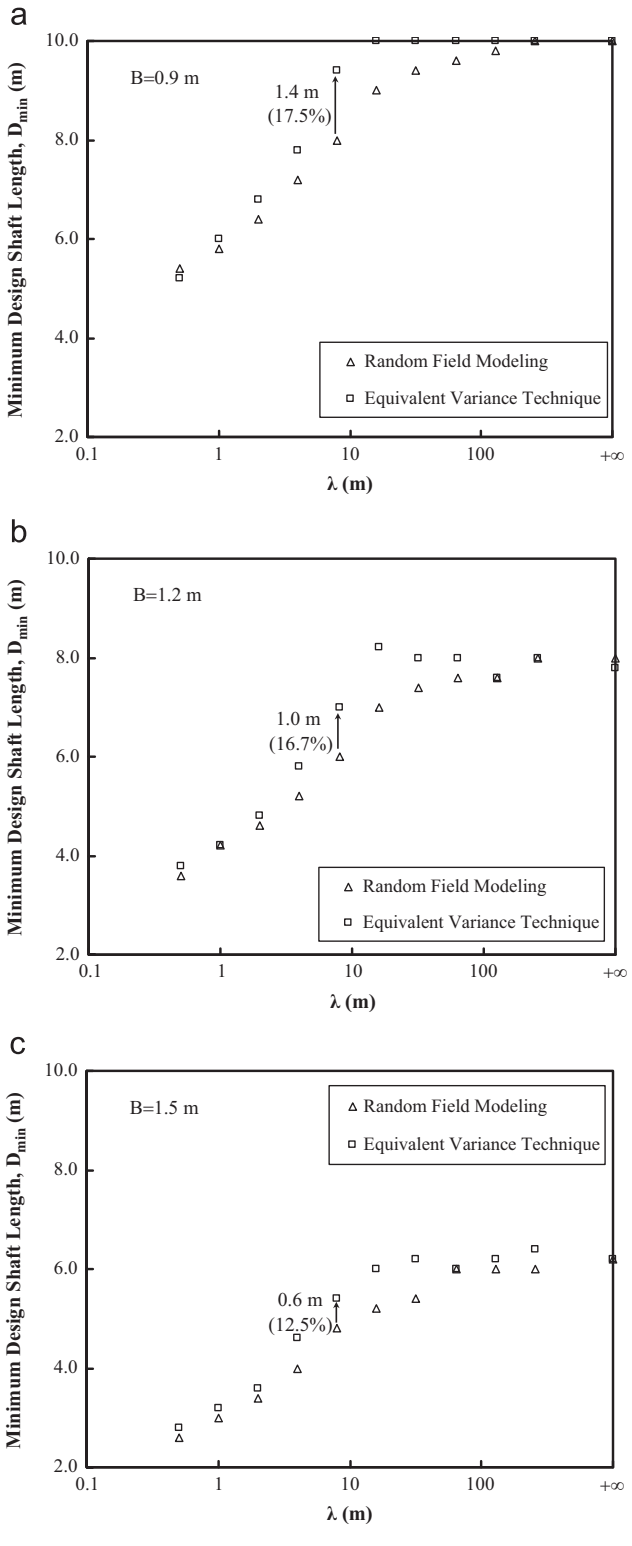

Fig. 10. Effects of indirect modeling of inherent spatial variability on feasible designs. (a) $B=0.9$ m (b) $B=1.2$ m and (c) $B=1.5$ m.

respectively. After FS_{uls} and FS_{sls} are obtained, the BD/FS_{min} is also calculated in the deterministic model worksheet.

A series of Subset Simulation runs are performed using the equivalent variance technique to model the inherent spatial variability together with different λ values varying from 0.5 m to $+\infty$, each of which has m=4, p_0=0.2, and N=15, 000. After each simulation, the values of p_f^{ULS} and p_f^{SLS} for different combinations of B and D are calculated using the RBD Add-In shown in Fig. 6 (b), and the feasible designs for ULS and SLS requirements are determined accordingly by comparing the values of p_f^{ULS} and p_f^{SLS} with $p_T^{ULS}=0.00069$ and $p_T^{SLS}=0.0047$, respectively.

Fig. 10 show the variation of D_{min} obtained using the equivalent variance technique to model inherent spatial variability for various λ values by squares. For comparison, Fig. 10 also includes the values of D_{min} obtained using RFM with the single exponential correlation structure (i.e., Eq. (1)) by triangles. The squares generally plot closely to triangles when $\lambda<1$ m or $\lambda>100$ m. The results obtained using the equivalent variance technique is in good agreement with those obtained using the RFM when $\lambda<1$ m or $\lambda>100$ m. On the other hand, when $\lambda>1$ m and $\lambda<100$ m, the squares generally plot above the triangles. This indicates that using the equivalent variance technique with the simplified form of the variance reduction function (i.e., Eq. (4)) leads to relatively conservative designs when λ varies from 1 m to 100 m. For example, when $\lambda=8$ m, the values of D_{min} for $B=0.9$ m, 1.2 m, and 1.5 m obtained using the equivalent variance technique with Eq. (4) are 1.4 m, 1.0 m, and 0.6 m greater than those obtained using the RFM, as shown in Fig. 10 (a), (b), and (c), respectively. Because the range of λ from 1 m to 100 m includes the typical ranges (e.g., from 2 m to 6 m by Phoon and Kulhawy , 1999a,b) of vertical scale of fluctuation of in-situ test data on strength parameters of soil reported in the geotechnical literature, using the equivalent variance technique with the simplified form of the variance reduction function in RBD might result in conservative designs of drilled shafts in design practice.

10. Selection of driving variable

Driving variable Y is a key factor that affects the generation of conditional samples of interest in Subset Simulation. In the expanded RBD approach, the conditional samples of interest are failure samples conditional on design parameters (e.g., B and D for drilled shafts, the width W_{sf} and length L_{sf} for spread foundations (Wang, 2011), and the embedded depth D_{spw} for sheet pile walls (Wang, 2013)). To yield design information for a wide range of design parameters, the driving variable needs to simultaneously drive the sampling space to failure domain and generate effectively failure samples with a wide range of design parameters. It is, therefore, recommended to define the driving variable as a combination of failure criterion (e.g., FS) and design parameters of interest (e.g., B and D in drilled shaft design, W_{sf} and L_{sf} in spread foundation design, and D_{spw} in sheet pile wall design). As several FS values (e.g., FS_{uls} and FS_{sls} in this study) might be calculated in the design, it is recommended that the minimum (i.e., FS_{min}) of these FS values is used to define Y.

This study defines the driving variable as $Y=BD/FS_{min}$. Subset Simulation generates samples with increasing values of the driving variable BD/FS_{min} as the level increases. The increase of BD/FS_{min} is attributed to two factors: decrease of the denominator FS_{min} and increase of the numerator BD. Thus, the effect of driving variable $Y=BD/FS_{min}$ on the sampling process is two-folded. On one hand, due to the

decrease of denominator FS_{min}, Subset Simulation drives the sampling space to failure domain with relatively small FS_{min} values that usually correspond to relatively small B and D values (see Eqs. (14)–(18)). On the other hand, because of the increase of the numerator BD, Subset Simulation generates samples with relatively large B and D values. The combined effects of FS_{min} and BD in the driving variable $Y=BD/FS_{min}$ improve the efficiency of generating failures samples that cover a wide range of B and D values, particularly those with relatively large values of B and D. Similar to the driving variable (i.e., BD/FS_{min}) defined in the drilled shaft design in this study, the driving variables for spread foundation design and sheet pile wall design can be defined as $W_{sf}L_{sf}/FS_{min}$ and D_{spw}/FS_{min}, respectively.

To illustrate the effect of driving variable, two Subset Simulation runs are performed with two different driving variables: one with $Y=BD/FS_{min}$ and the other with $Y=1/FS_{min}$. Defining driving variable as a function of failure criterion (e.g., $Y=1/FS_{min}$) is a common practice in Subset Simulation (e.g., Au et al., 2010). The uncertainty modeling and deterministic modeling in the two Subset Simulation runs follow those adopted in the illustrative example. Each simulation run has $m=4$, $p_0=0.2$, and $N=15{,}000$, and results in totally 63,000 samples.

Table 1 summarizes the failure samples generated in the two Subset Simulations. The Subset Simulation with $Y=1/FS_{min}$ generates 34704 ULS failure samples, among which 93.0% have $B=0.9$ m, 6.8% have $B=1.2$ m, and 0.2% have $B=1.5$ m. Since there are very few samples with $B=1.5$ m, it is difficult to accurately estimate failure probability for designs with $B=1.5$ m. In contrast, the Subset Simulation with $Y=BD/FS_{min}$ generates 25965 ULS failure samples. The percentage of ULS failure samples with $B=0.9$ m decreases to 84.7%, while the percentages of ULS failure samples with $B=1.2$ m and $B=1.5$ m increase to 14.2% and 1.1%, respectively. The simulation with $Y=BD/FS_{min}$ generates more ULS failure samples with relatively large B values (e.g., $B=1.2$ m and $B=1.5$ m) than the simulation with $Y=1/FS_{min}$. In addition, Table 1 shows that the maximum values (D_{max}) of D among the ULS failure samples at $Y=BD/FS_{min}$ are also larger than those at $Y=1/FS_{min}$. Similar observations are also found for the SLS failure samples summarized in Table 1. It is evident that using $Y=BD/FS_{min}$ leads to more failure samples with relatively large B and D values, and it is more appropriate to use $Y=BD/FS_{min}$ than $Y=1/FS_{min}$ in the proposed approach.

11. Summary and conclusions

This paper developed a RBD approach for drilled shafts, which integrates a Monte Carlo Simulation (MCS)-based RBD approach (i.e., the expanded RBD approach) with the random field theory to model, directly and explicitly, the inherent spatial variability of soil properties in RBD. The proposed approach is implemented in a commonly-available EXCEL spreadsheet environment by a package of worksheets and VBA functions/Add-Ins. The implementation is divided into three parts: a deterministic model worksheet, an uncertainty model worksheet, and a Subset Simulation and RBD Add-In. The uncertainty modeling and propagation by Subset Simulation and calculations of conditional failure probability for the expanded RBD are deliberately decoupled from the deterministic model worksheet for traditional foundation design calculation so they can proceed as an extension of the deterministic calculation in a non-intrusive manner. This effectively removes the hurdle of reliability computational algorithm and provides a user-friendly graphical user interface to practicing engineers.

To improve the efficiency and resolution at small probability levels, the proposed approach enhances the expanded RBD approach with an advanced MCS method called "Subset Simulation". Equations were derived for the integration of the expanded RBD approach and Subset Simulation. The proposed approach was illustrated through a drilled shaft design example. The results obtained from the proposed approach were validated against those obtained from the expanded RBD approach with direct MCS. Compared with the expanded RBD approach with direct MCS, the proposed approach requires much less random samples. Subset Simulation significantly improves the computational efficiency at small probability levels and enhances the expanded RBD approach in design situations with a small target failure probability.

With the aid of improved efficiency by the Subset Simulation, the proposed approach was applied to explore the effects of inherent spatial variability (including the scale of fluctuation and correlation structure) on the RBD of drilled shafts. It was shown that the scale of fluctuation λ affects feasible designs significantly. Ignoring spatial variability (i.e., $\lambda=+\infty$) leads to conservative designs at small probability levels, which happen to be of great interest in foundation designs. The results also showed that the correlation structure might have considerable effects on RBD of drilled shafts. The proposed approach

Table 1
Summary of failure samples generated using different driving variables.

Limit state	Driving variable, Y	Number of failure samples	Percentage of failure samples (%)			D_{max} (m)		
			$B=0.9$ (m)	$B=1.2$ (m)	$B=1.5$ (m)	$B=0.9$ (m)	$B=1.2$ (m)	$B=1.5$ (m)
ULS	$1/FS_{min}$	34,704	93.0	6.8	0.2	5.4	3.8	2.6
	BD/FS_{min}	25,965	84.7	14.2	1.1	6.6	4.8	3.2
SLS	$1/FS_{min}$	44,700	84.9	12.5	2.6	8.2	5.4	4.4
	BD/FS_{min}	38,889	74.8	20.4	4.8	9.4	7.0	5.4

accounts for the effects of both the scale of fluctuation and correlation structure in RBD of drilled shafts in a direct and explicit manner. Note that although a stationary random field is applied in this study to model the inherent spatial variability of soil properties, the proposed approach is applicable for general choices of uncertainty modeling of soil properties, such as non-stationary random fields to model the inherent spatial variability of soil properties. The uncertainty model that is deemed appropriate shall be used in the expanded RBD, provided that sufficient data is available for such modeling.

The proposed approach was applied to evaluate the effect of indirect modeling of inherent spatial variability using the equivalent variance technique and the simplified form of the variance reduction function in RBD. It was found using the equivalent variance technique with the simplified form of the variance reduction function leads to relatively conservative designs at small probability levels when the scale of fluctuation λ falls within the typical range of in-situ test data on strength parameters of soil reported in the geotechnical literature.

In addition, the selection of driving variable in Subset Simulation for the expanded RBD was discussed. It is recommended to define the driving variable as a combination of failure criterion (e.g., FS_{min}) and design parameters of interest (e.g., B and D in drilled shaft design). BD/FS_{min} is found to be a proper choice for drilled shaft design.

Acknowledgments

The work described in this paper was supported by a Strategic Research Grant from City University of Hong Kong (Project Number 7002838). The financial support is gratefully acknowledged.

References

Ang, H.S., Tang, W.H., 2007. Probability Concepts in Engineering: Emphasis on Applications to Civil and Environmental Engineering, 2nd ed John Wiley and Sons, New York.

Au, S.K., 2005. Reliability-based design sensitivity by efficient simulation. Comput. Struct. 83 (14), 1048–1061.

Au, S.K., Beck, J.L., 2001. Estimation of small failure probabilities in high dimensions by Subset Simulation. Probab. Eng. Mech. 16 (4), 263–277.

Au, S.K., Beck, J.L., 2003. Subset Simulation and its application to probabilistic seismic performance assessment. J. Eng. Mech. 129 (8), 1–17.

Au, S.K., Cao, Z., Wang, Y., 2010. Implementing advanced Monte Carlo simulation under spreadsheet environment. Struct. Saf. 32, 281–292.

Baecher, G.B., Christian, J.T., 2003. Reliability and Statistics in Geotechnical Engineering. John Wiley and Sons, New Jersey.

Cao, Z., Wang, Y., 2013. Bayesian approach for probabilistic site characterization using cone penetration tests. J. Geotech. Geoenviron. Eng. 139 (2), 267–276.

Chen, J.J., Zhang, L., 2013. Effect of spatial correlation of cone tip resistance on the bearing capacity of piles. J. Geotech. Geoenviron. Eng. 139 (3), 494–500.

Christian, J.T., Ladd, C.C., Baecher, G.B., 1994. Reliability applied to slope stability analysis. J. Geotech. Eng. 120 (12), 2180–2207.

El-Ramly, H., Morgenstern, N.R., Cruden, D.M., 2002. Probabilistic slope stability analysis for practice. Can. Geotech. J. 39, 665–683.

Fenton, G.A., 1999a. Estimation for stochastic soil models. J. Geotech. Geoenviron. Eng. 125 (6), 470–485.

Fenton, G.A., 1999b. Random field modeling of CPT data. J. Geotech. Geoenviron. Eng. 125 (6), 486–498.

Fenton, G.A., Griffiths, D.V., 2007. Reliability-based Deep Foundation Design, Probabilistic Applications in Geotechnical Engineering, Geotechnical Special Publication no. 170, pp. 1–12.

Fenton, G.A., Griffiths, D.V., 2003. Bearing capacity prediction of spatially random c-ϕ soils. Can. Geotech. J. 40 (1), 54–65.

Fenton, G.A., Griffiths, D.V., 2002. Probabilistic foundation settlement on spatially random soil. J. Geotech. Geoenviron. Eng. 128 (5), 381–390.

Fenton, G.A., Naghibi, M., 2011. Geotechnical resistance factors for ultimate limit state design of deep foundations in frictional soils. Can. Geotech. J. 48, 1742–1756.

Griffiths, D.V., Fenton, G.A., 2009. Probabilistic settlement analysis by stochastic and random finite-element methods. J. Geotech. Geoenviron. Eng. 135 (11), 1629–1637.

Griffiths, D.V., Fenton, G.A., 2004. Probabilistic slope stability analysis by finite elements. J. Geotech. Geoenviron. Eng. 130 (5), 507–518.

Huang, J., Griffiths, D.V., Fenton, G.A., 2010. System reliability of slopes by RFEM. Soils Found. 50 (3), 343–353.

Honjo, Y., Kikuchi, Y., Shirato, M., 2010. Development of the design codes grounded on the performance-based design concept in Japan. Soils Found. 50 (6), 983–1000.

Honjo, Y., 2008. Monte Carlo simulation in reliability analysis. In: Phoon, K. K. (Ed.), Chapter 4 in Reliability-Based Design in Geotechnical Engineering: Computations and Applications. Taylor & Francis, London.

Kasama, K., Whittle, A.J., Zen, K., 2012. Effect of spatial variability on the bearing capacity of cement-treated ground. Soils Found. 52 (4), 600–619.

Kim, J.M., Sitar, N., 2013. Reliability approach to slope stability analysis with spatially correlated soil properties. Soils Found. 53 (1), 1–10.

Klammler, H., McVay, M., Horhota, D., Lai, P., 2010. Influence of spatially variable side friction on single drilled shaft resistance and LRFD resistance factors. J. Geotech. Geoenviron. Eng. 136 (8), 1114–1123.

Kulhawy, F.H., 1996. From Casagrande's 'Calculated Risk' to reliability-based design in foundation engineering. Civil Eng. Pract. 11 (2), 43–56.

Kulhawy, F.H., 1991. Drilled Shaft Foundations. In: Fang, H.Y. (Ed.), Chapter 14 in Foundation Engineering Handbook 2nd ed Van Nostrand Reinhold, New York, pp. 537–552.

Li, D.Q., Qi, X.H., Zhou, C.B., Phoon, K.K., 2013. Effect of spatial variability of shear strength parameters that increase linearly with depth on reliability of infinite slopes. Structural Safety, (Accepted).

Li, C.-C., Der Kiureghian, A., 1993. Optimal discretization of random fields. J. Eng. Mech. 119 (6), 1136–1154.

Luo, Z., Atamturktur, S., Cai, Y., Juang, C.H., 2012. Simplified approach for reliability-based design against basal-heave failure in braced excavations considering spatial effect. J. Geotech. Geoenviron. Eng. 138 (4), 441–450.

Mitchell, J.K., Soga, K., 2005. Fundamentals of Soil Behavior. John Wiley and Sons, New Jersey.

Naghibi, M., Fenton, G.A., 2011. Geotechnical resistance factors for ultimate limit state design of deep foundations in cohesive soils. Can. Geotech. J. 48, 1729–1741.

Phoon, K.K., Kulhawy, F.H., 1999a. Characterization of geotechnical variability. Can. Geotech. J. 36 (4), 612–624.

Phoon, K.K., Kulhawy, F.H., 1999b. Evaluation of geotechnical property variability. Can. Geotech. J. 36 (4), 625–639.

Phoon, K., K., Kulhawy, F.H., Grigoriu, M.D., 1995. Reliability-based Design of Foundations for Transmission Line Structures. Electric Power Research Institute, Palo Alto, CA (Report TR-105000).

Phoon, K.K., Quek, S.T., An, P., 2003. Identification of statistically homogeneous soil layers using modified Bartlett statistics. J. Geotech. Geoenviorn. Eng. 129 (7), 649–659.

Santoso, A., Phoon, K.K., Quek, S.T., 2009. Reliability Analysis of Infinite Slope using Subset Simulation, Contemporary Topics in In Situ Testing, Analysis, and Reliability of Foundations, Geotechnical Special Publication no. 186, pp. 278–285.

Schmertmann, J.H., 1967. Guidelines for use in the Soils Investigation and Design of Foundations for Bridge Structures in the State of Florida, Research Bulletin 121-A, Florida Department of Transportation, Gainesville, Fla.

Sivakumar Babu, G.L., Mukesh, M.D., 2004. Effect of soil variability on reliability of soil slopes. Geotechnique 54 (5), 335–337.

Teixeira, A., Honjo, Y., Correia, A.G., Henriques, A.A., 2012. Sensitivity analysis of vertically load pile reliability. Soils Found. 52 (6), 1118–1129.
Vanmarcke, E.H., 1983. Random Fields: Analysis and Synthesis. MIT Press, Cambridge.
Vanmarcke, E.H., 1977. Probabilistic modeling of soil profiles. J. Geotech. Eng. 103 (11), 1127–1246.
Vesić, A.S., 1975. Bearing Capacity of Shallow Foundations. In: Winterkorn, H.F., Fang, H.Y. (Eds.), Chapter 3 in Foundation Engineering Handbook. Van Nostrand Reinhold, New York, pp. 121–147.
Wang, Y., 2013. MCS-based probabilistic design of embedded sheet pile walls. Georisk 7 (3), 151–162.
Wang, Y., 2011. Reliability-based design of spread foundations by Monte Carlo simulations. Geotechnique 61 (8), 677–685.
Wang, Y., Au, S.K., Kulhawy, F.H., 2011a. Expanded reliability-based design approach for drilled shafts. J. Geotech. Geoenviron. Eng. 137 (2), 140–149.
Wang, Y., Cao, Z., Au, S.K., 2011b. Practical reliability analysis of slope stability by advanced Monte Carlo simulations in spreadsheet. Can. Geotech. J. 48 (1), 162–172.
Wang, Y., Au, S.K., Cao, Z., 2010a. Bayesian approach for probabilistic characterization of sand friction angles. Eng. Geol. 114 (3–4), 354–363.
Wang, Y., Cao, Z., Au, S.K., 2010b. Efficient Monte Carlo simulation of parameter sensitivity in probabilistic slope stability analysis. Comput. Geotech. 37, 1015–1022.
Wang, Y., Kulhawy, F.H., 2008. Reliability index for serviceability limit state of building foundations. J. Geotech. Geoenviron. Eng. 134 (11), 1587–1594.
Zhang, J., Zhang, L.M., Tang, W.H., 2011. Kriging numerical models for geotechnical reliability analysis. Soils Found. 51 (6), 1169–1177.
Zhang, L., Chen, J.J., 2012. Effect of spatial correlation of standard penetration test (SPT) data on bearing capacity of driven piles in sand. Can. Geotech. J. 49, 394–402.
Zhang, L.M., Chu, L.F., 2009a. Calibration of methods for designing large-diameter bored piles: Ultimate limit state. Soils Found. 49 (6), 883–895.
Zhang, L.M., Chu, L.F., 2009b. Calibration of methods for designing large-diameter bored piles: serviceability limit state. Soils Found. 49 (6), 897–908.